Materials Advances

ROYAL SOCIETY OF CHEMISTRY

COMMUNICATION

View Article Online
View Journal | View Issue

Cite this: *Mater. Adv.*, 2025, 6, 6257

Received 2nd June 2025,
Accepted 30th July 2025

DOI: 10.1039/d5ma00579e

rsc.li/materials-advances

Control of cancer cell phenotypes *via* supramolecular hydrogels: the role of extracellular matrix stiffness

Virginie Baylot,[a] Bruno Alies,[a] Palma Rocchi[b] and Philippe Barthélémy *[a]

Malignant cell lines are frequently used as a model to understand cancer and identify potential new treatments. However, maintaining the initial cancer cell phenotypes in a culture remains an important challenge and strongly impacts the proper evaluation of novel therapeutic approaches. The mechanical properties of the extracellular matrix (ECM) are known to strongly impact the fate and phenotype of cells. Herein, we report a tunable artificial ECM based on supramolecular gels, allowing the control of cancer cell phenotypes.

As one of the important components of the tumor microenvironment, the modification of, and in particular the increase in, ECM stiffness is a remarkable feature of cancers.[1] During tumor formation, cancer cells increase ECM stiffness, which, in turn, has an impact on their characteristics and fate. Many cancer cells have been cultured in Matrigel, a complex biological system extracted from the secretion of *Engelbreth–Holm–Swarm* mouse sarcoma cells and enriched for extracellular matrix proteins.[2] Despite its massive use in laboratories, Matrigel™ is a complex mixture with more than one thousand components,[3] which induces batch-to-batch variabilities. Moreover, this ECM may not contain the proper components, cues and mechanical properties adapted to the cancer cells of interest. Given these limitations, there is an urgent need to develop an artificial ECM, allowing the improvement of 3D cancer cell culture methods.[4] Supramolecular gels for cell culture are three-dimensional networks formed by reversible supramolecular interactions, such as hydrogen bonding, van der Waals forces, and π–π stacking, rather than covalent bonds.[5] These materials provide supportive scaffolds that mimic the extracellular matrix (ECM), allowing for better cell attachment, growth, and differentiation compared with traditional two-dimensional systems.[6]

Supramolecular gels based on glycosyl-nucleo-bola-amphiphiles (GNBAs) are emerging as an attractive class of an artificial ECM in cell culture owing to their key features, including biocompatibility, dynamic properties and modularity.[7] These gels can be easily tailored in terms of composition, mechanical properties, and degradation rates, enabling customization for specific cell types or applications.[8,9] Furthermore, the reversible nature of supramolecular interactions in a gel can alter its properties in response to environmental stimuli, which can be beneficial for studying cellular behavior.[10] Owing to their intrinsic properties, GNBAs can be used for a variety of applications, including drug delivery[8] and tissue engineering, offering an innovative approach for experimental research.

Tissues in the human body comprise diverse extracellular matrix (ECM) components, giving rise to a broad range of elastic moduli (Fig. 1). Each tissue exhibits a characteristic mechanical profile that supports its physiological role. For example, brain tissue is among the softest (~0.1–1 kPa), facilitating neuronal plasticity and dynamic cell–matrix interactions, whereas mineralized bone is orders of magnitude stiffer (gigapascal range), enabling structural support and protection of internal organs (Fig. 1).[12] ECM stiffness regulates cellular behavior[13] and contributes to tissue homeostasis, pathology, and disease progression, including cancer.[14]

To further explore and expand the use of GNBA biomaterials, we exposed different cancer cell lines, including prostate cancer (PCa) PC-3 and LNCaP lineages into GNBA supramolecular hydrogels. The LNCaP cell line was initially established from a lymph node metastasis of a patient with metastatic PCa,[15] and the PC-3 cell line was initiated from a bone metastasis of a patient with prostatic adenocarcinoma.[16] Since these cell lines come from different tissues, their actual local environment features different stiffness. Lymph node tissues (LNCaP) exhibit elastic modulus G' in the range of a few kPa (5 to 9 kPa),[17,18] whereas prostate cancer metastasis to bone (PC3) shows a G' higher than 1 MPa.[19] However, to form the secondary tumor in the bone,[20] prostate cancer cells have to first interact with collagen-rich ECM,[21] such as the one found in osteoid-like tissues (~30 to 45 kPa). Hence, as a proof of concept, we hypothesised that modulating gel stiffness in the 0.2–30 kPa range could maintain the initial phenotype of

[a] *University of Bordeaux, INSERM U1212, UMR CNRS 5320, F-33076 Bordeaux, France. E-mail: philippe.barthelemy@inserm.fr*
[b] *Aix Marseille Univ, CNRS, CINAM, ERL INSERM U 1326, CERIMED, Marseille, France*

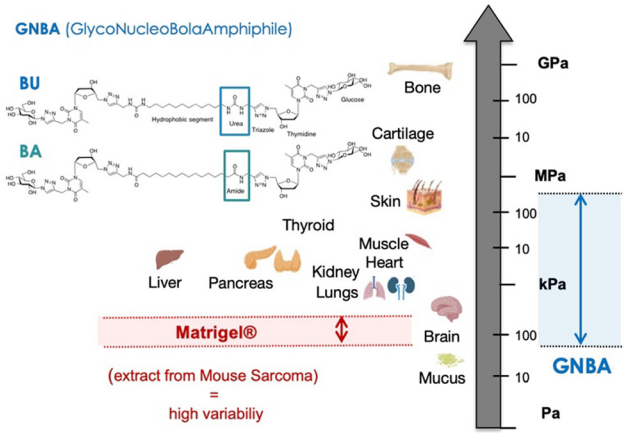

Fig. 1 (Left) Chemical structures of the two glycosyl-nucleo-bola-amphiphiles (GNBAs, BU for bisurea in blue and BA for bisamide in green) used in this study. (Right) Illustration showing the elastic moduli of different organs and tissues. The stiffest tissues of a body are teeth and bones ($G' >$ 1 GPa), and the lungs and brain are among the softest ($G' >$ 100 Pa). Matrigel (in red) shows stiffness values G' around 400 Pa,[11] whereas elastic moduli of GNBA supramolecular gels can be modulated from 100 Pa to 100 kPa[10] (in blue). The stiffness of PC3 and LNCaP cellular environments is shown on this scale.

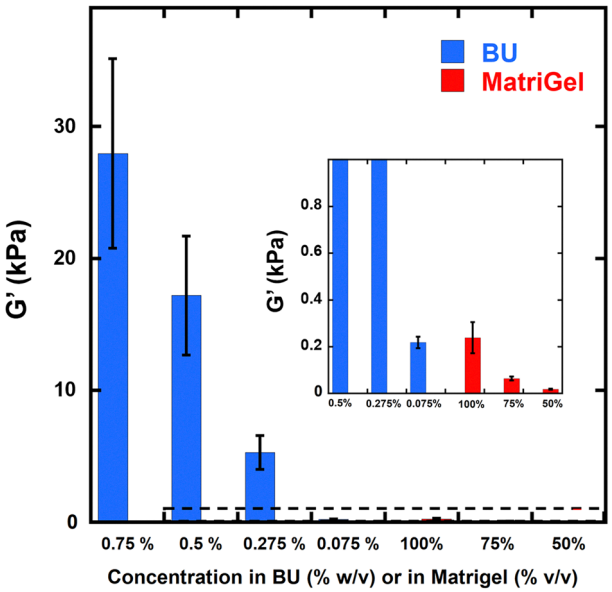

Fig. 2 Elastic moduli (G') values recorded at a sweep frequency of 1 Hz. G' of GNBA (BU) based supramolecular gels (blue) *versus* matrigel (red) are reported at different concentrations (BU % w/v, Matrigel % v/v).

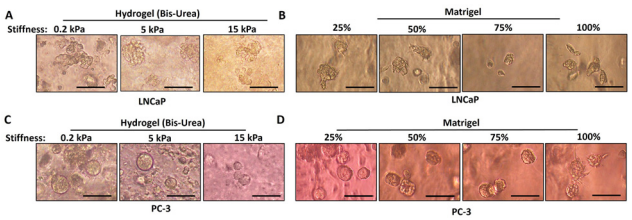

Fig. 3 LNCaP and PC-3 cells formed spheroids when cultured in GNBA-based matrix and Matrigel™ at different stiffness. Representative images of the spheroids derived from LNCaP (A and B) and PC-3 (C and D) cell lines, were acquired with a phase-contrast microscope at the 10× magnification, scale bars: 100 μm.

cancer cells. Previous studies have shown that changes in cell phenotype arising from external environment conditions are irreversible.[22,23] We thus explored cell behavior modifications due to ECM stiffness in these two PCa cell lines that were derived from tumors progressing in tissues with different stiffness.

First, the mechanical behaviors of GNBA-based gels and Matrigel were investigated by oscillatory rheology at different concentrations in RPMI culture media (Fig. 2). In the case of GNBA gels, the observed values for the storage modulus at a sweep frequency of 1 Hz were dependent on the GNBA concentrations. At high 0.75% (w/v), the supramolecular gels feature a G' of 28 kPa ± 7 kPa, whereas a G' of 0.2 kPa ± 30 Pa was observed at a concentration of 0.075% w/v, illustrating the large elastic modularity of GNBA gels (Fig. 2 and Fig. S4). Notably, very low G' values were measured for the Matrigel samples (from 0.2 kPa ± 70 Pa at 100% to <0.02 kPa ± 5 Pa at 50%), indicating both very low stiffness and weak elastic modularity of the Matrigel materials (Fig. 2 and Fig. S5, S6).

Next, PC-3 and LNCaP cell lines were cultured in GNBA supramolecular hydrogels with different stiffness values (0.2, 5, 15 and 30 kPa) mimicking lymph nodes, normal prostate, prostate tumor and bone tissues stiffness, respectively (Fig. 3). Matrigel™, standard 3D culture ECM, which displays low stiffness values at all the concentrations (100, 75, 50 and 25%) was used to embed the PCa cells (Fig. 3). PC-3 and LNCaP cells formed spheroids in both Matrigel™ and GBNA-based hydrogels 7 days after they were embedded in both matrices with no significant differences in the number and size of spheroids (Fig. 3). After 32 days, LNCaP and PC-3 cells were collected, and the impact of ECM stiffness on the cellular phenotype was investigated. LNCaP cells that grew in soft matrices (GBNA hydrogel at 0.2 kPa and Matrigel™) maintained their original migratory and proliferative abilities, when compared to the parental cell line (Fig. 4 and Fig. S3A, B). Meanwhile, LNCaP cultured in stiff substrates display reduced capacities to proliferate (30% of reduction, $P \leq 0.001$, ***) and migrate (30 to 40% of decrease, $P \leq 0.001$, ***) (Fig. 4A, C and Fig. S1).

In contrast, PC-3 cells show reduced proliferation and migration efficiency when cultured in soft ECM (GBNA hydrogel at 0.2 kPa and Matrigel™) compared to the parental cell line or cells cultured in stiff matrices (hydrogel stiffness values of 15 and 30 kPa) (Fig. 5 and Fig. S3C, D). Proliferation rates were reduced by 18% ($P \leq 0.001$, ***) and we observed a 33% decrease of migration abilities ($P \leq 0.01$, **) for PC-3 cells that grew in 0.2 kPa GBNA-based gels, compared to their parental counterparts (Fig. 5A, C and Fig. S2). Interestingly, we showed that PC-3 cells cultured in Matrigel™ lose the original cell line features, illustrated by a 20 to 40% of proliferative capacities reduction and a migration efficiency drop of 25 to 43% ($P \leq$ 0.01, **, $P \leq 0.001$, ***, Fig. 5B, D and Fig. S2). These results demonstrate that Matrigel™, for which the stiffness cannot be tuned depending on the cellular or tumor model, is not

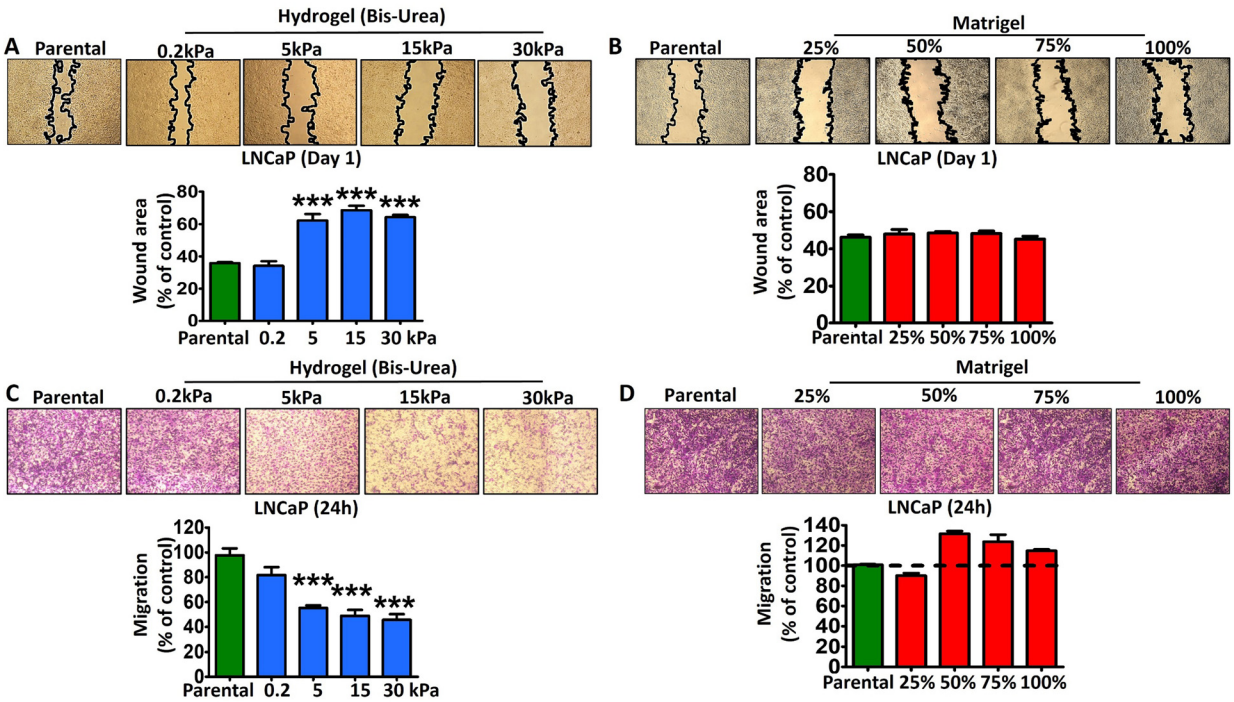

Fig. 4 LNCaP migration and proliferation capacities vary according to the stiffness of matrices. (A) and (B) Proliferation rates of LNCaP cultured in GBNA supramolecular hydrogels at different concentrations 0.2, 5, 15 and 30 kPa (A) and in Matrigel™ at 25, 50, 75 and 100% (B) evaluated by a wound healing assay. Images of the wounds (representative pictures are shown in the first line) were acquired 24 hours after the scratch was created (n = 12 per condition) and analysed using ImageJ (n = 3 wells per condition). (C) and (D) LNCaP cells were cultured in GBNA-based hydrogels (C) and Matrigel™ (D), and migration abilities were investigated using Transwell assays (n = 3 wells per condition). Representative images of migrated cells stained with crystal violet are shown in the first line. For quantification (graph bars shown in second line), crystal violet was solubilized in ethanol and the absorbance at 555 nm was measured. For all the *in vitro* experiments, the parental LNCaP cell line was used as the reference. Statistically significant differences between the conditions of culture were determined by analysis of variance (one-way ANOVA). p-Values of Tukey's *post hoc* analyses are presented. *$P < 0.05$, **$P < 0.01$ and ***$P < 0.001$.

adapted to grow cells or tumors that were isolated from stiff tissues.

In conclusion, we have shown that supramolecular gels applied to cancer 3D cell cultures allow adaptation of the elastic properties of the artificial ECM to the native tumor environment. As demonstrated for PCa cell lines (PC-3 and LNCaP), the proliferation and migration properties are impacted by the artificial ECM stiffness. LNCaP cells maintained their original phenotype in both weak GNBA gels and Matrigel™, mimicking their native environment. However, PC-3 cells require ECM featuring higher stiffness, lose their native phenotype in the weak Matrigel™, demonstrating that controlling the ECM stiffness in cell cultures is required for maintaining the native phenotypes. 3D cell cultures are often developed to mimic in an accurate fashion the original tumor, for both drug screening and tumor characteristic studies. Such models need to maintain the native clinical features over time to be relevant. In this study, we clearly demonstrate the importance of adapting the ECM stiffness to the tumor or cell models to keep their native phenotypes. Overall, the GNBA supramolecular gels feature key characteristics required for 3D cell-cultures, including (i) modularity of the elastic moduli over a large range of values compared to Matrigel™ (Fig. 1), (ii) ease of use (see SI Movie) thanks to their intrinsic supramolecular nature, (iii) non-toxicity and (iv) their applicability to different cells.[6] The possibility of modulating the viscoelastic properties of supramolecular gels is a promising tool in cell culture, providing a more realistic environment for cells compared to traditional methods.

Methods

Cell culture

Human prostatic cell lines LNCaP (castration-sensitive prostate cancer cells) and PC-3 (castration-resistant prostate cancer cells) were cultured in RPMI-1640 (Roswell Park Memorial Institute) and DMEM (Dulbecco's Modified Eagle's Medium), respectively, supplemented with 10% of fetal bovine serum (FBS) at 37 °C in 5% CO_2.

Spheroids culture

LNCaP and PC-3 cells were embedded in gels (BU) based on the protocol of El Hamoui *et al.*[10] Briefly, the adequate volume of the culture media (RPMI + FBS for LNCaP and DMEM + FBS for PC-3) was added to specific amounts of the gelator molecule powder to obtain the desired ECM stiffness (from 0.2 to 30 kPa). The mixture was then heated at 80 °C for 15 minutes and left at room temperature for 4–5 additional minutes to reduce the temperature before adding the cells. The LNCaP and PC-3 cells

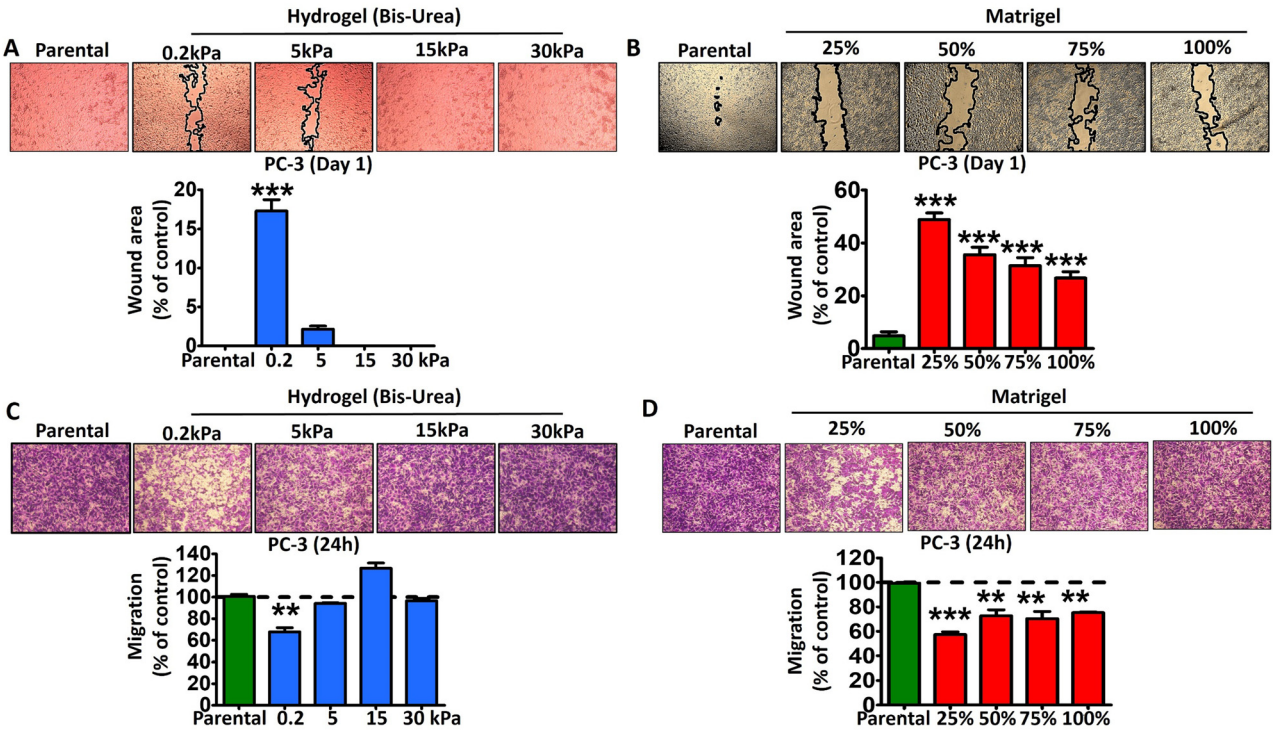

Fig. 5 PC-3 display reduced migration and proliferation efficiencies when cultured in soft matrices. A and B- Proliferation capacities of PC-3 cultured in the specified substrates–GBNA supramolecular hydrogels at different stiffness values of 0.2, 5, 15 and 30 kPa (A) and in Matrigel™ at 25%, 50%, 75% and 100% (B)—were evaluated by *in vitro* scratch assay. Images of the wounds (first line, n = 12 per condition) were acquired at 0 and 24 hours after the scratch was created and analysed using ImageJ (n = 3 wells per condition). (C) and (D) PC-3 cells were cultured in GBNA based hydrogels (C) and Matrigel™ (D), and migration abilities were investigated using Transwell assays (n = 3 wells per condition). Representative images of migrated cells stained with crystal violet are showed on the first line. For quantification (graph bars), crystal violet was eluted from cells in ethanol and the absorbance at 555 nm was measured. For all the *in vitro* experiment, the parental PC-3 cell line was used as the reference. Statistically significant differences between the conditions of culture were determined by analysis of variance (one-way ANOVA). p-Values of Tukey's *post-hoc* analyses are presented. $^{*}P < 0.05$, $^{**}P < 0.01$ and $^{***}P < 0.001$.

were counted with an automated cell counter (Cell Countess 3, Invitrogen) and encapsulated in the gel (BU) material at a final concentration of 50 000 cells per mL. The prostate cancer cells were embedded in Matrigel™ at the same final concentration. Matrigel™ was used either as such (pure, 100%) or diluted with adequate cell media at different Matrigel/Media ratios including 3/1 (75%), 1/1 (50%), 1/3 (25%). The mixture of cells/material was transferred to 96 well plates (100 μL per well) and left at 37 °C for 10 minutes to allow the gelation of the matrices. Finally, 200 μL of culture media was added to each well. The first spheroids appeared after 7 days and were left in culture for 35 days. The culture media was refreshed twice a week.

Dissociation of spheroids

After 35 days in a 3D culture, LNCaP and PC-3 spheroids were isolated and disrupted into single-cell suspensions. The spheroids embedded in BU hydrogels and Matrigel™ were dissociated by pipetting the mixture cells/gel up and down in 1 ml of cold PBS. The cells were spun down by centrifugation and washed twice in cold PBS. The cells were counted and plated at the same concentration in 6-well plates for 2 days before performing the different *in vitro*-based assays.

Microscopy

LNCaP and PC-3 cells cultured in 3D were imaged at Day 14 using a phase-contrast microscope. All images were obtained with a 10× objective.

Migration assays

LNCaP and PC-3 cells were cultured in 3D at specified conditions. Parental cell lines that were never cultured in 3D were used as controls. The migration assays were performed using Thermo Scientific™ Nunc™ polycarbonate cell culture inserts (membrane pore size of 8 μm) in 24-well plates. 75 000 cells per well were plated onto the transwell upper chamber in 200 μL of serum-free culture media and 500 μL of complete media was added onto the bottom chamber. After 24 hours, the cells were washed twice in PBS, and fixed in PBS + 4% of paraformaldehyde (PFA) for 15 minutes at RT. After 2 washing steps in PBS, the non-migrated cells on the upper surface of the transwells were gently removed with cotton swabs. The migrated cells on the bottom surface of the transwells were stained with 0.2% (w/v) crystal violet for 5 minutes. Migrated cells were observed with a phase-contrast microscope. For the quantification, crystal violet coloration was solubilized in ethanol for

5 minutes, transferred to clean 96-well plates and the optical density was read at 555 nm using a plate reader.

Wound healing assays

LNCaP and PC-3 cells were cultured in 3D at specified conditions. Parental cell lines that were never cultured in 3D were used as controls. PC-3 and LNCaP cells were seeded at a concentration of 360×10^5 and 500×10^5 cells per well in a 24-well plate, respectively. The cell monolayer was scraped in a straight line to create a "scratch" with a p200 pipette tip. Debris and the smooth edge of the scratch were removed by washing the cells twice with PBS. The images of the wounds were acquired on a phase-contrast microscope.

Statistical analysis

Results were analyzed and represented as mean ± SEM. Statistical analyses were performed using GraphPad Prism 6 software (GraphPad Software, Inc). The one-way ANOVA followed by Tukey-Kramer *post hoc* test was used to compare the means between the different conditions of culture. Results with $P < 0.05$ were considered statistically significant and are indicated by *, $P < 0.05$; **, $P < 0.01$; and ***, $P < 0.001$.

Rheology experiments

Rheological measurements were carried out on a Malvern Kinexus Pro+ rheometer with steel cone-plate geometry (diameter: 20 mm). The lower plate was equipped with a Peltier temperature control system. A solvent trap was used to ensure homogeneous temperature and to prevent water evaporation. BU in cell medium (RPMI + FBS) was heated at 85 °C, and was deposited on the motionless disk of the rheometer, and then the cone-plate was set and the gel could rest and cure between the disks. All rheology experiments were performed at 37 ± 0.05 °C. G' moduli indicated in Fig. 2 were taken at a frequency of 1 Hz (ω = 6.283 rad s^{-1}) at a strain of 0.5% and error bars represent a standard deviation of moduli during frequency sweep (data shown in Fig. S4 and S5). Strain amplitude sweep experiments are displayed in Fig. S6.

Author contributions

P. B., V. B. and B. A. conceived and led the project. Experiments were performed by B. A. and V. B., with assistance from P. R. for cell experiments. P. B. wrote the manuscript with input from all other authors.

Conflicts of interest

There are no conflicts to declare.

Data availability

The data supporting this article have been included as part of the SI. Supplementary information available: Details of the proliferative capacities of cancer cells and their ability to form colonies, viscoelastic measurements of Matrigel and supramolecular gels. See DOI: https://doi.org/10.1039/d5ma00579e

Notes and references

1 J. Huang, L. Zhang, D. Wan, L. Zhou, S. Zheng, S. Lin and Y. Qiao, *Signal Transduction Targeted Ther.*, 2021, **6**, 153.
2 H. K. Kleinman and G. R. Martin, *Semin. Cancer Biol.*, 2005, **15**, 378–386.
3 C. S. Hughes, L. M. Postovit and G. A. Lajoie, *Proteomics*, 2010, **10**, 1886–1890.
4 L. Rijns, M. B. Baker and P. Y. W. Dankers, *J. Am. Chem. Soc.*, 2024, **146**, 17539–17558.
5 C. Wu, W. Liao, Y. Zhang and Y. Yan, *Biomater. Sci.*, 2024, **12**, 4855–4874.
6 T. Saydé, O. E. Hamoui, B. Alies, G. Bégaud, B. Bessette, S. Lacomme, P. Barthélémy, G. Lespes, S. Battu and K. Gaudin, *J. Chromatogr. A*, 2024, **1736**, 465393.
7 M. A. Ramin, L. Latxague, K. R. Sindhu, O. Chassande and P. Barthélémy, *Biomaterials*, 2017, **145**, 72–80.
8 N. D. Bansode, K. R. Sindhu, C. Morel, M. Rémy, J. Verget, C. Boiziau and P. Barthélémy, *Biomater. Sci.*, 2020, **8**, 3186–3192.
9 J. Baillet, A. Gaubert, J. Verget, L. Latxague and P. Barthelemy, *Soft. Matter.*, 2020, **16**, 7648–7651.
10 O. El Hamoui, T. Saydé, I. Svahn, A. Gudin, E. Gontier, P. Le Coustumer, J. Verget, P. Barthélémy, K. Gaudin, S. Battu, G. Lespes and B. Alies, *ACS Biomater. Sci. Eng.*, 2022, **8**, 3387–3398.
11 S. S. Soofi, J. A. Last, S. J. Liliensiek, P. F. Nealey and C. J. Murphy, *J. Struct. Biol.*, 2009, **167**, 216–219.
12 D. E. Discher, P. Janmey and Y. Wang, *Science*, 2005, **310**, 1139–1143.
13 O. Chaudhuri, J. Cooper-White, P. A. Janmey, D. J. Mooney and V. B. Shenoy, *Nature*, 2020, **584**, 535–546.
14 M. J. Paszek, N. Zahir, K. R. Johnson, J. N. Lakins, G. I. Rozenberg, A. Gefen, C. A. Reinhart-King, S. S. Margulies, M. Dembo, D. Boettiger, D. A. Hammer and V. M. Weaver, *Cancer Cell*, 2005, **8**, 241–254.
15 J. S. Horoszewicz, S. S. Leong, E. Kawinski, J. P. Karr, H. Rosenthal, T. M. Chu, E. A. Mirand and G. P. Murphy, *Cancer Res.*, 1983, **43**, 1809–1818.
16 M. E. Kaighn, K. S. Narayan, Y. Ohnuki, J. F. Lechner and L. W. Jones, *Invest. Urol.*, 1979, **17**, 16–23.
17 J.-W. Jung, H. Je, S.-K. Lee, Y. Jang and J. Choi, *Front. Bioeng. Biotechnol.*, 2020, **8**, 979.
18 H. N. Jung, I. Ryoo, S. Suh, Y. H. Lee and E. Kim, *Magn. Reson. Med. Sci.*, 2024, **23**, 49–55.
19 M. S. Molla, D. R. Katti and K. S. Katti, *J. Biomech.*, 2021, **114**, 110142.
20 P. Clézardin, *Jt., Bone, Spine*, 2017, **84**, 677–684.
21 B. A. Roeder, K. Kokini, J. E. Sturgis, J. P. Robinson and S. L. Voytik-Harbin, *J. Biomech. Eng.*, 2002, **124**, 214–222.
22 Z. Liu, L. Wang, H. Xu, Q. Du, L. Li, L. Wang, E. S. Zhang, G. Chen and Y. Wang, *Adv. Sci.*, 2020, **7**, 1903583.
23 X. Tang, Y. Zhang, J. Mao, Y. Wang, Z. Zhang, Z. Wang and H. Yang, *Beilstein J. Nanotechnol.*, 2022, **13**, 560–569.